

The dynamical evolution of massive black hole binaries - II. Self-consistent N-body integrations.

Gerald D. Quinlan¹ and Lars Hernquist²

¹Dept. of Physics and Astronomy, Rutgers University, PO Box 849, Piscataway NJ 08855
(Present address: 1055 Bay St., #1503, Toronto, Canada M5S 3A3)

²Lick Observatory, University of California, Santa Cruz CA 95064

August 30, 2018

Abstract

We use a hybrid N-body program to study the evolution of massive black hole binaries in the centers of galaxies, mainly to understand the factors affecting the binary eccentricity, the response of the galaxy to the binary merger, and the effect of loss-cone depletion on the merger time. The scattering experiments from paper I showed that the merger time is not sensitive to the eccentricity growth unless a binary forms with at least a moderate eccentricity. We find here that the eccentricity can become large under some conditions if a binary forms in a galaxy with a flat core or with a radial bias in its velocity distribution, especially if the dynamical friction is enhanced by resonances as suggested by Rauch and Tremaine (1996). But the necessary conditions all seem unlikely, and our prediction from paper I remains unchanged: in most cases the eccentricity will start and remain small. As a binary hardens it ejects stars from the center of a galaxy, which may explain why large elliptical galaxies have weaker density cusps than smaller galaxies. If so, the central velocity distributions in those galaxies should have strong tangential anisotropies. The wandering of a binary from the center of a galaxy mitigates the problems associated with loss-cone depletion and helps the binary merge.

1 Introduction

The formation of massive black hole (BH) binaries follows from two widely held assumptions: that galaxies merge and that many galaxies contain central BHs. The evolution of these binaries is relevant to a number of problems in extragalactic astronomy. They have been proposed to explain the bends in jets from active galaxies (Begelman et al., 1980; Roos, 1988; Roos et al., 1993; Gaskell, 1996), and the difference between radio-loud and radio-quiet active galaxies (Wilson and

Colbert, 1995). Multiple mergers of BH binaries can lead to the buildup of massive central BHs (Hut and Rees, 1992), although if the binaries do not merge quickly the BHs can be ejected through three-body interactions (Xu and Ostriker, 1994; Valtonen, 1996), a process that has been proposed to explain the double radio lobes of active galaxies (Saslaw et al., 1974; Valtonen et al. 1994). The double nucleus of the nearby galaxy M31 (Lauer et al., 1993) could be a BH binary in the making, although Tremaine (1995) has proposed a plausible model that requires only one BH. If binary mergers are frequent they will be the most interesting source of gravitational radiation for the planned space-based detector LISA (Haehnelt, 1994; Bender et al., 1995). Lastly, the evolution of BH binaries may explain why the density profiles of elliptical galaxies fall into two classes, with small galaxies having strong density cusps and large galaxies having weaker cusps (Ebisuzaki et al., 1991; Faber et al., 1996).

The relevance of BH binaries to all of these problems depends on how long it takes for dynamical friction (resulting from star-BH interactions) and gravitational radiation to cause the binaries to merge. The merger time is difficult to compute because the hardening of the binary changes the structure of the galaxy, which in turn changes the hardening rate. The back-of-the-envelope calculations of Begelman et al. (1980) have now been supplemented with numerical results from three-body scattering experiments (Roos, 1981; Mikkola and Valtonen, 1992) and full N-body experiments (e.g., Ebisuzaki et al., 1991; Makino, 1997), yet several big uncertainties remain. The eccentricity evolution has been subject to much debate, the most recent contribution being that of Rauch and Tremaine (1996) who argue that resonant interactions between the BHs and the stars can cause a rapid growth in the eccentricity if the velocity distribution has a radial anisotropy. This would cause gravitational radi-

ation to become important early in the evolution and would help the binaries merge. Another uncertainty has been loss-cone depletion, the depletion of the low-angular-momentum stars that can interact with the binary, which lowers the hardening rate and lengthens the merger time. Because of the uncertainties one can find papers in the recent literature making widely different predictions for merger times in typical galaxies, ranging from $\lesssim 10^8$ yr (e.g., Makino and Ebisuzaki, 1994) to well over a Hubble time (e.g., Rajagopal and Romani, 1995; Valtonen, 1996).

In paper I (Quinlan, 1996) we presented results from a new set of three-body scattering experiments as a first step towards resolving the uncertainties. We computed the hardening rate, the eccentricity growth rate, and the rate at which a binary ejects stars, and derived formulas to fit the dependence of the rates on the hardness and mass ratio of the binary. One of the main results was that the eccentricity of a hard binary grows only slowly as the binary hardens, and that the growth does not change the merger time by much unless the binary starts with at least a moderate eccentricity, say $e \gtrsim 0.5$ (this had been demonstrated for equal-mass binaries by Mikkola and Valtonen, 1992). But in deriving these results we made some simplifying assumptions that may not be applicable to real galaxies: we assumed a homogeneous, isotropic galaxy core with a Maxwellian velocity distribution, and we ignored the change in the core caused by the binary. We thus could not study the response of the galaxy and the depletion of loss-cone orbits in a self-consistent manner, nor could we study the dependence on the initial density profile or on anisotropies in the velocity distribution.

To improve upon the scattering experiments we have developed a hybrid N-body program that is well suited to studying the evolution of BH binaries in models for elliptical galaxies, including models with cusps and anisotropies. In this paper we describe the design and performance of the program and then use it to study the factors affecting the eccentricity, the response of the galaxy to the binary hardening, and the effect of loss-cone depletion on the hardening rate. We pay special attention to the convergence of the results with the number of particles and to some differences between the N-body results and the predictions from paper I.

We ignore some complications that may be important for real galaxies. We consider only spherical or nearly spherical galaxies, and ignore disks or triaxial components of the potential. A disk will alter the frictional force on the BHs, possibly dragging them into the disk plane, and a triaxial component will help the merger by increasing the number of stars that can interact with the binary. We also ignore gas, which

can help the merger by accreting onto the BHs or by applying a frictional force to the BHs. We wish to understand the simple problem with purely stellar-dynamical processes first before we add complications. The neglected complications should not matter for binaries in gas-poor, nearly spherical galaxies like M87.

2 Computational methods

2.1 The N-body program

N-body programs are usually designed to solve problems of one of two types: collisional or collisionless. In collisional problems the evolution depends in an essential way on close encounters between the stars. These problems require accurate integrations with the exact $1/r^2$ force law, and are usually solved with high-order integrators. In collisionless problems the evolution depends not on close encounters between the stars but on the collective response of the system to changes in the potential. These problems require a large number of particles to suppress spurious relaxation, and are usually solved with a low-order integrator (e.g., leapfrog) and a fast, approximate method for computing the forces. The BH-binary problem does not fit neatly into either of these types. The binary evolves because of close encounters between the BHs and the stars, which must be integrated accurately, but the galaxy evolves because of the collective response of the stars to changes in the potential, and the number of stars must be large, both to suppress relaxation and to satisfy the requirement that the stars be much less massive than the BHs.

It is not surprising then that both types of N-body programs have been used for the problem. Governato et al. (1994) used a tree program with the leapfrog integrator and a large softening length to study the merger of King models containing central BHs, with 16,000 particles per galaxy. Their program was good for the galaxy merger and the early stages of the binary evolution, but not for the late stages, which they did not study. Mikkola and Valtonen (1992) used Aarseth's NBODY1 program to study the evolution of a BH binary at the center of a Plummer model with 10,000 particles. NBODY1 uses a fourth-order integrator with individual stepsizes, which makes it better than a tree program for the late stages of the evolution, but it computes the forces by direct summation, which is slow. Mikkola and Valtonen assumed a fixed Plummer potential when computing the forces between the stars, which made the integrations go faster but at the price of ignoring the self-consistent response of the galaxy. Self-consistent integrations of galaxy mergers with central BHs using over 10^5 particles per

galaxy were done with a direct-summation program by Makino and Ebisuzaki (1996) and Makino (1997), but on a GRAPE-4 supercomputer, whose speed of 100–150 Gflops is beyond the reach of general-purpose computers.

Our hybrid N-body program works well for both the collisional and collisionless aspects of the BH-binary problem. We call it SCFBDY because it combines parts from the SCF program of Hernquist and Ostriker (1992) and the NBODY programs of Aarseth (1994). We describe here the main features of the program and their advantages for the BH-binary problem; a more technical description is given in the appendix.

The program moves the BHs and stars according to different equations of motion (we use lower-case letters for the stars, upper-case for the BHs, and set $G = 1$):

$$\ddot{\vec{R}}_i = \sum_j \frac{M_j(\vec{R}_j - \vec{R}_i)}{|\vec{R}_j - \vec{R}_i|^3} + \sum_k \frac{m_k(\vec{r}_k - \vec{R}_i)}{(|\vec{r}_k - \vec{R}_i|^2 + \epsilon_i^2)^{3/2}}, \quad (1)$$

$$\ddot{\vec{r}}_k = \sum_j \frac{M_j(\vec{R}_j - \vec{r}_k)}{(|\vec{R}_j - \vec{r}_k|^2 + \epsilon_j^2)^{3/2}} - \sum_{n,l,m} A_{nlm} \nabla \Phi_{nlm} \quad (2)$$

The BHs interact with the other BHs and with the stars through the $1/r^2$ force (a softening parameter is added for the BH-star interactions). The stars interact with the BHs through the $1/r^2$ force, but with the other stars through an expansion of the potential with coefficients A_{nlm} that are updated with time self-consistently. By using the Φ_{nlm} basis functions of Hernquist and Ostriker (1992) we can fit the potentials of most elliptical-galaxy models adequately with a small number of coefficients—a dozen is often enough for spherical galaxies. Phinney and Villumsen (Phinney 1994) split the equations for the BH-binary problem in a manner similar to our equations (1) and (2), but used a different expansion for the potential and used the leapfrog integrator to move the particles. We move the particles with individual stepsizes (sometimes differing by as much as a factor of 10^6) using one of Aarseth’s (1994) fourth-order integrators—the NBODY1 integrator for the stars, and NBODY2 or NBODY6 for the BHs. Our program thus combines the integration accuracy of a direct-summation program with the speed of a SCF type of program.

The program does have some limitations. It does not vectorize or parallelize as well as the pure SCF program. It modifies two-body interactions between the stars by replacing the potential by a smooth approximation, and hence cannot be used to study the diffusion of stars into the loss cone by two-body relaxation. (Programs that do not replace the potential by a smooth approximation commit the opposite error for the BH-binary problem: they give a diffusion

rate larger than would occur in a real galaxy, because they cannot use as many stars as there are in a real galaxy.) And the program requires a central point about which the potential can be expanded, at least in the simple version used here with only one expansion center, which means that it cannot be used to study the galaxy mergers that lead to galaxies with more than one central BH. We ignore that stage of the evolution.

2.2 Initial conditions and units of measurement

We used three simple, isotropic galaxy models for our experiments in this paper, as well as some anisotropic models that will be described later. The first of the simple models is the Plummer model, with a density

$$\rho(r) = \frac{3M}{4\pi d^3} \left(1 + \frac{r^2}{d^2}\right)^{-5/2}. \quad (3)$$

The Plummer model is easy to set up and interpret, but is a poor model for real galaxies: they are much more concentrated, many with densities that continue rising to the innermost observable radius (Crane et al., 1993; Ferrarese et al., 1994; Forbes et al., 1995; Lauer et al., 1995). We therefore used two models with density cusps from the family considered by Dehnen (1993) and Tremaine et al. (1994):

$$\rho(r) = \frac{3 - \gamma}{4\pi} \frac{Md}{r^\gamma (r + d)^{4-\gamma}}. \quad (4)$$

We used the models with $\gamma = 1$ and $\gamma = 2$, which are the models of Hernquist (1990) and Jaffe (1983). The “ γ models” fit density profiles of elliptical galaxies reasonably well if the length scale d is chosen to be close to the effective radius. The inner parts of elliptical galaxies can be fit better by Zhao’s (1996) formula, $\rho(r) \sim r^{-\gamma} (r^{1/\alpha} + d)^{(\beta-\gamma)\alpha}$, with β typically in the range 2–3 (the length scale d , or “break radius”, is much smaller than the effective radius in these fits), which is similar to the fitting formula used by Byun et al. (1996). The difference between Zhao’s models and the γ models is unimportant for our work because we are mainly interested in the region $r < d$ where the models are the same. We truncate the models at $r = 300d$.

To increase the statistical resolution near the center, and to help satisfy the requirement that the stars be much less massive than the BHs, we give the stars a mass spectrum, with the masses decreasing towards the center as

$$m \sim r_p^\lambda, \quad (5)$$

with r_p the initial pericenter of the star and λ an exponent, usually in the range 0.5–1.0 (Sigurdsson et

al., 1995). In a Jaffe model with $\lambda = 0.75$, for example, about 40% of the stars have $r/d < 0.1$ and 20% have $r/d < 0.01$, whereas the corresponding percentages for an equal-mass model are 10% and 1%. The mass spectrum does not lead to mass segregation, because the potential is smooth with our program and the segregation time is long. We impose minimum and maximum masses, typically differing by a factor of 1000, so that the masses do not become arbitrarily small or large at small and large radii.

The BHs are treated as point masses obeying Newtonian gravity. The detected massive BHs in real galaxies have a mean mass of 0.002–0.003 (in units of the bulge mass), although there is a scatter of at least one order of magnitude about this mean (Kormendy and Richstone, 1995). It is difficult to use small BHs in the experiments because the dynamical-friction time for those is long and because we need the stars to be much less massive than the BHs. We therefore use BHs somewhat larger than occur in real galaxies, $m_{\text{bh}}/M \simeq 0.01$, and vary their masses to determine how the results scale with the mass. The scaling is not important for the eccentricity results, which are not sensitive to the masses (except for the results on resonant friction), but it is important for the response of a galaxy to the binary evolution. Our masses are not that unrealistic given that our galaxy models have less mass at large radii than a real galaxy would have (if we interpret $r = d$ as the break radius).

The initial condition for our BHs are of two types. In the first we start the BHs symmetrically about the origin in one of the galaxy models described above, at $r \simeq d$. We assume that the BHs arrived there after a galaxy merger, or after being dragged in from the halo of the galaxy. After a merger the BHs would probably be surrounded by clusters of bound stars, but we ignore those (our potential expansion has trouble resolving small clumps of stars away from the center). In the second we start a galaxy with one large BH at the center, surrounded by a cluster of bound stars, and allow a smaller BH with no cluster of bound stars to sink in from $r \simeq d$. The second type of initial condition is more realistic than the first, but the first is adequate for answering some questions and is easier to use than the second, because in the second the central BH and the stars surrounding it require small stepsizes right from the start of the integration.

We present the N-body results in a system of units in which $G = M = 1$, with M the mass of the galaxy without the BHs. We usually choose the length scale so that $E = -1/4$, with E the energy of the initial galaxy without the the BHs. The length scales d for the Plummer and γ models are then $3\pi/16$ and $1/(5-2\gamma)$, and the half-mass radius and the density and dynamical time at that radius are all of order unity. We specify

the softening for the BH-star interactions by either the softening length ϵ or the softening velocity

$$v_\epsilon = \sqrt{Gm_{\text{bh}}/\epsilon}. \quad (6)$$

As in paper I, we define the binary orbital velocity V_{bin} by

$$V_{\text{bin}} = \sqrt{GM_{12}/a}, \quad (7)$$

with $M_{12} = m_1 + m_2$.

3 A sample integration

We shall describe one N-body experiment in detail to explain our assumptions, integration procedure, and method of data analysis, and to identify some of the questions to be studied later. We also use this experiment to test the sensitivity of the results to the integration parameters and the number of particles.

The problem that we consider is the hardening of an equal-mass binary at the center of a Jaffe model. The galaxy was represented by 10^5 particles with a mass exponent $\lambda = 0.75$. The BHs had masses $m_1 = m_2 = 0.01$, and were started on nearly circular orbits at (\vec{r}, \vec{v}) and $(-\vec{r}, -\vec{v})$, with $r = 0.5$. We integrated the orbits for 80 time units with an accuracy parameter $\eta = 0.005$, a softening velocity $v_\epsilon = 16$, and a spherical potential expansion (with $n_{\text{max}} = 18$, $l_{\text{max}} = 0$) whose coefficients were updated every $\Delta t = 0.005$; the integration took five days of cpu time on a DEC 250-4/266 AlphaStation. The program regularized the orbits at time $t = 17.85$. The total energy was conserved to about one part in 100.

The integration results are shown in Figure 1. The semimajor axis a and eccentricity e were computed from the BH coordinates and velocities by the usual formulas for a Kepler orbit, ignoring the interaction between the BHs and the stars. The eccentricity remained small ($e \lesssim 0.1$) and is not shown in the figure. The semimajor axis is shown in panel (b). The passage of $1/a$ through zero marks the time when the BHs become bound, $t = 6.15$, at which the separation between the BHs is $r = 0.063$. A BH binary becomes hard once its semimajor axis shrinks to $a_{\text{h}} = Gm_2/4\sigma^2$ (Quinlan, 1996), with σ the one-dimensional dispersion near the center but outside the Keplerian rise around the BHs. For the Jaffe model, $1/a_{\text{h}} = 200$ ($\sigma^2 = 1/2$). The hardening slows down noticeably after $1/a$ reaches about 500, because the binary has by then ejected many stars and has reduced the central density. But the hardening does not stop, because the binary does not remain at the center: it wanders around and is thus able to interact with new stars. This is apparent from the plot of the center-of-mass radius in panel (a).

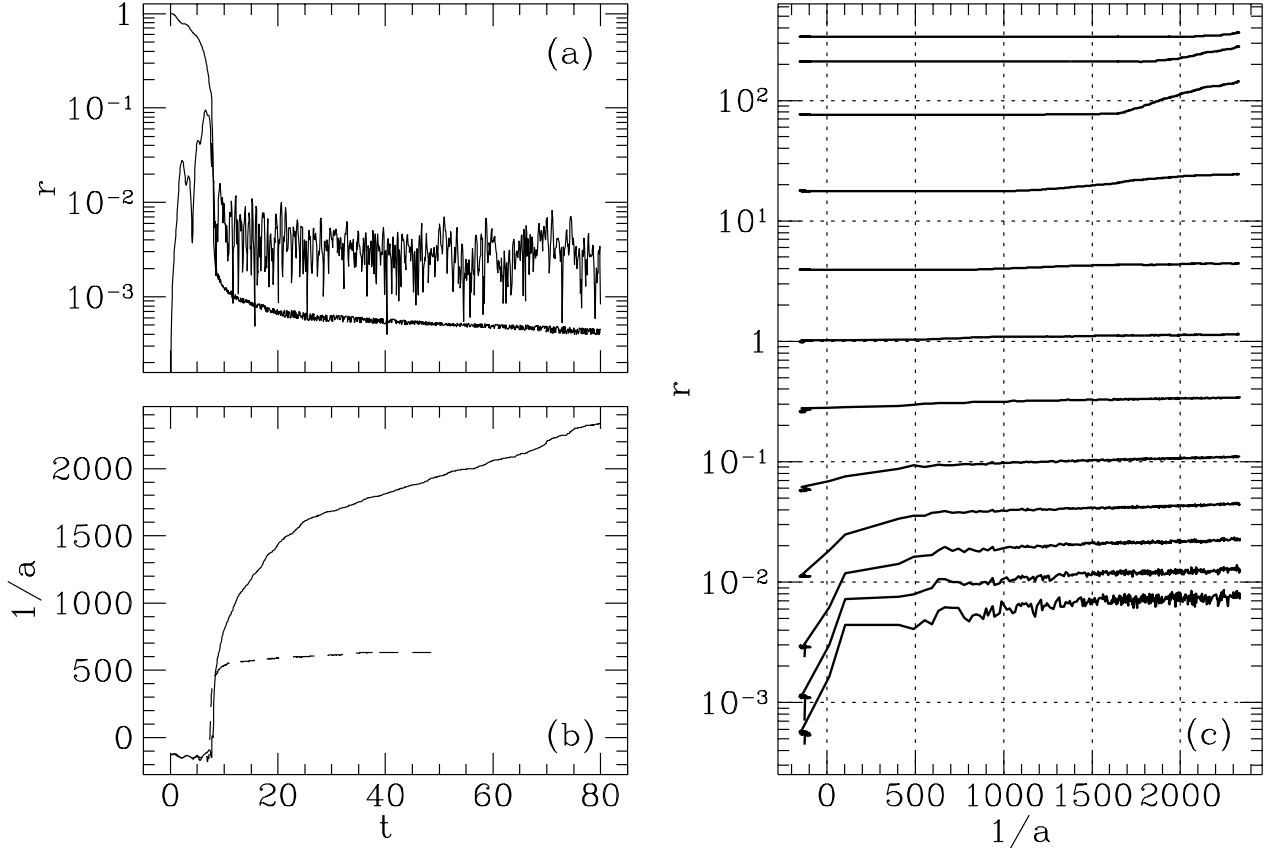


Figure 1: Binary evolution in a Jaffe model. Two equal-mass BHs ($m_1 = m_2 = 0.01$) were started on nearly circular orbits at (\vec{r}, \vec{v}) and $(-\vec{r}, -\vec{v})$, with $r = 0.5$. The panels show (a) the separation between the BHs (the lower line towards the end) and between their center of mass and the origin, (b) the semimajor axis, and (c) the radii containing fixed percentages of the galaxy mass: 0.008 (bottom line), 0.04, 0.2, 1, 5, 20, 50, 80, 95, 99, 99.8, and 99.96 (top line). The dashed line in panel (b) is from an integration in which the center of mass of the binary was fixed at the origin.

To check the importance of wandering we repeated the integration with a constraint force applied to keep the center of mass of the binary fixed at the origin. We did this by moving the BHs with the same stepsizes and by replacing the forces \vec{F}_1 and \vec{F}_2 on the BHs at each step by $\vec{F}_1 - \vec{F}_{\text{cm}}$ and $\vec{F}_2 - \vec{F}_{\text{cm}}$, with $\vec{F}_{\text{cm}} = (m_1\vec{F}_1 + m_2\vec{F}_2)/M_{12}$. With this constraint force the hardening stopped after $1/a$ reached about 650—see the dashed line in panel (b). A series of integrations like this with different binary masses showed that the hardening stops when the mass in stars that can approach within a of the center drops to a small fraction of the binary mass. For the Jaffe model the final, “loss-cone” separation a_{lc} therefore varies linearly with the binary mass, $a_{\text{lc}} \sim M_{12}$. This differs from the prediction of Begelman et al. (1980), but is similar to the predictions made by Roos (1981). When the binary is free to wander the hardening does not stop; we shall say more about this later.

We stopped the integration at $t = 80$ because it was

becoming slow, owing to the small stepsizes of the BHs. In a real galaxy gravitational radiation would at some point cause the BHs to merge. The time at which that would happen in our experiment depends on the physical mass and length scales, which we have not specified. Our neglect of gravitational radiation is justified during most of the evolution because the importance of radiation turns on suddenly—the timescales for hardening by three-body scattering and by radiation vary as $\sim 1/a$ and $\sim a^4$. Our goal is to integrate the Newtonian equations far enough that we can predict how the evolution would continue until the point at which radiation becomes important. For the applications that we are interested in—BHs of mass 10^8 – $10^9 M_\odot$ in a large galaxy like M87, or BHs of mass 10^5 – $10^6 M_\odot$ in a smaller, denser galaxy like M32—radiation becomes important after the semimajor axis shrinks by a factor of 10–50 beyond $a = a_h$ (Quinlan, 1996). In our integration the semimajor axis shrank by a factor of 12 beyond $a = a_h$, which might have

been enough.

Panel (c) shows how the galaxy expands as the stars absorb energy from the BHs. This starts when the BHs first sink into the center, before they become bound, but most of it occurs after the binary forms and begins hardening. The expansion appears to slow down near the end, but that is mainly because the figure uses a linear scale for $1/a$ and a logarithmic scale for r . Near the end the outer parts of the galaxy begin expanding too, because of the stars that the binary has ejected.

To test the dependence of the results on the integration parameters we repeated the integration with different choices of η , v_ϵ , Δt , n_{\max} , and l_{\max} . None of the changes had a significant effect on the binary evolution unless a parameter was changed to an unreasonable value, such as a softening velocity lower than the orbital velocity of the binary at the end of the integration ($V_{\text{bin}} = 6.8$), or a value of η or Δt so large that energy conservation was grossly violated. Even adding non-spherical terms to the potential by changing l_{\max} from 0 to 2 hardly affected the binary, because the galaxy remained nearly spherical throughout the integration. The parameters that we used thus seem adequate for our purposes.

To test the dependence on the number of particles we compared results from integrations using 6250, 25000, and 10^5 particles, using both equal-mass particles ($\lambda = 0$) and particles with a mass spectrum ($\lambda = 0.75$). For each (λ, N) combination we performed three integrations, with the orbits of the BHs started in the XY, YZ, and ZX planes; the difference between them is a measure of the noise level. The results are summarized in Figure 2.

The eccentricity is noisy when N is low, especially with the models with equal-mass particles, because the eccentricity of a hard binary gets perturbed only by a small fraction of the stars—those that have close encounters with the binary. In the models with a mass spectrum that fraction is larger and the eccentricity is less noisy. The convergence of the eccentricities towards $e \simeq 0.05$ as N rises in panels (d), (e), and (f) suggests that it is the correct answer.

The semimajor axis is not as noisy as the eccentricity. Even with only 6250 particles the integrations starting from the three orbital planes give nearly the same hardening rate. But there is a systematic decrease in the rate as N rises from 6250 to 10^5 . A similar decrease was observed by Makino (1997), who proposed two explanations: two-body relaxation and the wandering of the binary from the center of the galaxy. Since our program suppresses two-body relaxation, the decrease most likely results from interactions between the stars and the center of mass of the binary. As N rises the perturbations that the binary experiences become less noisy and the binary wanders

less from the center. It therefore reduces the density near the center more and its hardening slows down. The wandering amplitude cannot be made arbitrarily small by raising N , as it could if the binary were a single particle, because the restoring force that keeps the binary at the center grows weaker as the central density goes down. There is therefore an N value above which the hardening stops decreasing with N , about 10^5 for the experiment considered here: panel (i) shows that the hardening rate with $N = 2 \times 10^5$ is the same as with $N = 10^5$. For smaller BHs the wandering continues growing to larger N values. The mass spectrum affects the wandering less than it affects the eccentricity, because the center of mass gets perturbed by all the stars near the center, not just by the stars having close encounters with the binary. The mean hardening rates found with equal-mass particles differed only slightly (they were larger) from those found with a mass spectrum.

This sample integration has thus shown that our program can integrate binaries accurately in large N-body systems without great expense, but also that the results have to be extrapolated with care before they can be applied to real galaxies. The value of N can easily be the largest source of error if it is small. For the eccentricity it is possible with the help of a mass spectrum to choose N large enough to suppress the noise—the value required is inversely proportional to the masses of the BHs. For the semimajor axis this is more difficult, because the mass spectrum does not help as much, but it is still possible if the BHs are large. The main uncertainty that the value of N introduces is in the hardening rate; it does not affect the response of the galaxy (except right at the center) if that is plotted versus the binary semimajor axis as it is in panel (c) of Figure 1.

4 The effect of wandering on the hardening and ejection rates

Our N-body program can be used both to test the predictions from our 3-body scattering experiments and to study dynamical processes that could not be explored with those experiments. In this section we test the predictions for the hardening and mass-ejection rates. There are several reasons for suspecting that these rates may differ in the N-body experiments. The most obvious is that the stellar distribution evolves along with the binary in the N-body experiments, whereas in the scattering experiments it is assumed to be fixed. When the low-angular-momentum parts of the distribution get depleted the hardening slows

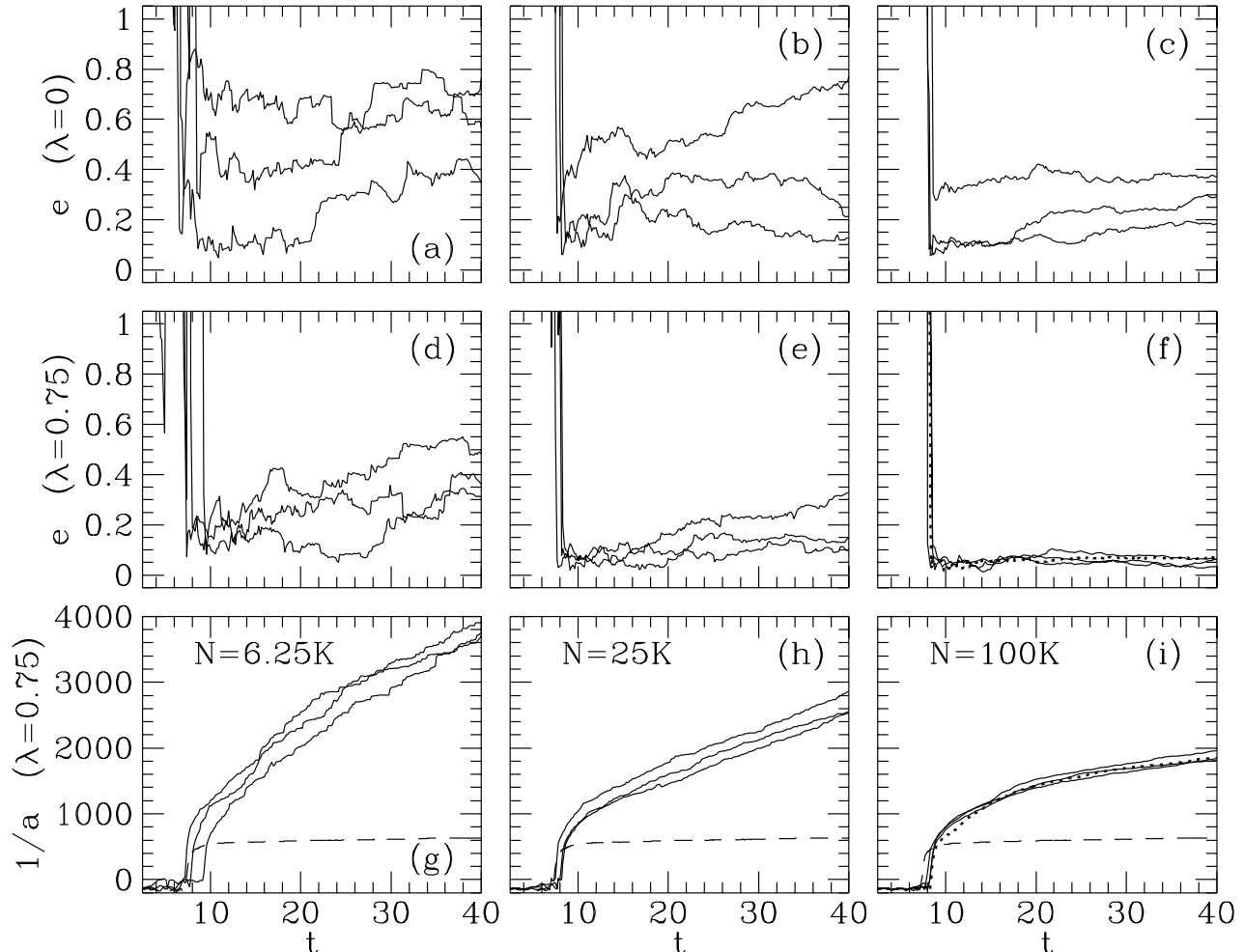


Figure 2: Dependence of the binary evolution on the number of particles (N), for the experiment shown in Fig. 1. The left, middle, and right columns show the eccentricity and semimajor axis computed with $N/10^3 = 6.25, 25$, and 100 . The integrations in the top row used equal-mass particles ($\lambda = 0$); those in the bottom two rows used a mass spectrum ($\lambda = 0.75$). For each combination of λ and N the integration was done three times with three different orbital planes for the initial orbits of the BHs. The dotted lines in panels (f) and (i) are from an integration with $N = 2 \times 10^5$ and $\lambda = 0.75$. The dashed lines in the bottom row are from panel (b) of Fig. 1.

down. But differences can occur even in the absence of loss-cone depletion, because in the N-body experiments the stars are influenced by forces from both the binary and the galaxy, not just from the binary as in the scattering experiments, and because in the N-body experiments the binary does not remain fixed in space. We argue here that the wandering of the binary increases the ejection rate by about a factor of two.

The evidence for this is shown in Figure 3. In panel (b) we plot the ejected mass as a function of the binary orbital velocity during integrations of binaries in a Jaffe model (with $N = 10^5$, and with the binaries started as was the binary in Fig. 1). We computed the ejected mass at time t from $M_{\text{ej}}(t) =$

$M(r_*, 0) - M(r_*, t)$, with r_* the radius at which $\rho(r_*, t)/\rho(r_*, 0) = 0.95$. The five lines in panel (b) are about the same within the uncertainties; we take the dashed-dotted line as the mean N-body result (integrations with other N values gave similar results). We also plot the prediction from our 3-body scattering experiments, computed from

$$M_{\text{ej}}(a)/M_{12} = C + \int_a^\infty \frac{da}{a} J(a), \quad (8)$$

where C , which we set to 0.6, is to allow for the mass that gets removed when the BHs first sink into the center, and J is the 3-body ejection rate (in what follows we speak of $dM_{\text{ej}}/dV_{\text{bin}}$ loosely as though it were the ejection rate). In computing the 3-body prediction

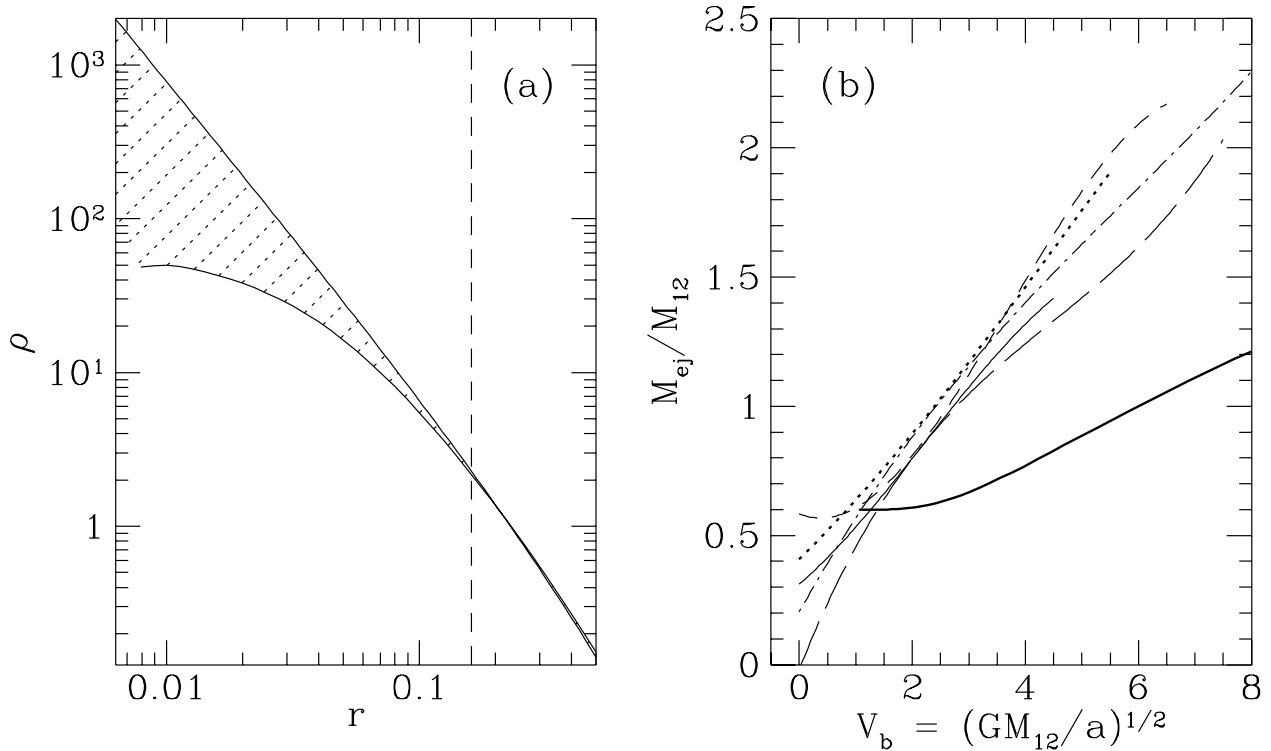


Figure 3: Ejected mass during integrations of equal-mass binaries in a Jaffe model. (a) Stellar density at the start (top line) and end (bottom line) of the integration of Fig. 1. The dashed line is drawn at $r = r_*$; the shaded region indicates the ejected mass. (b) Ejected mass versus binary orbital velocity from integrations like that of Fig. 1 but with $m_1 = m_2 = 0.04$ (solid line), 0.02 (dotted), 0.01 (short dashed), 0.005 (long dashed), and 0.0025 (dashed dotted); the heavy solid line is the prediction from the scattering experiments of paper I.

we assumed a Maxwellian velocity distribution with $\sigma^2 = 1/2$, and, as we did in paper I, we counted stars as ejected if they get expelled from the binary with a velocity larger than $v_{ej} = \sqrt{12}\sigma$. Although there is some uncertainty in the appropriate values for C , σ , and v_{ej} , it is too small to explain the factor-of-two difference in the slopes of the N-body and 3-body ejection curves near the end of the integration. Similar differences were found from integrations with galaxy models with other γ values.

A simple thought experiment suggests that the wandering of the binary can account for a large part of the difference. Suppose the binary moves so fast that incoming stars can interact with it only once before it moves out of their reach. For some stars this will not matter, but for others, which would experience multiple interactions before getting expelled if the binary were not wandering, it will. The cross sections in Figure 4 of paper I show that the hardening rate is sensitive to these multiple scattering events. Additional calculations from those cross sections show that the hardening rate for a hard, equal-mass binary gets reduced by a factor of 7.5 when stars are allowed to

interact with the binary only once, whereas dM_{ej}/dt gets reduced by at most a factor of two. This thought experiment is admittedly unrealistic, because in reality the binary will not be moving as fast as we have assumed, but the qualitative conclusion drawn from it should be correct: wandering will decrease the hardening rate more than dM_{ej}/dt , and hence will increase the ejection rate when it is expressed as dM_{ej}/dV_{bin} or $dM_{ej}/d\ln(1/a)$.

To test this conclusion we compared the ejection rates from N-body integrations with the binaries free to wander with those from integrations with the center of mass of the binaries fixed at the origin (as was described in Sec. 3). We added a small triaxial perturbation to the potential (the same for both sets of integrations) to allow more stars to reach the center, for otherwise in the integrations with the center of mass fixed the hardening would not have continued far enough for us to make a fair comparison. The ejection rate was close to the 3-body prediction when the center of mass was fixed, but not when it was free; the difference was again about a factor of two.

If our explanation is correct, the hardening rate in

the N-body experiments should be lower than was predicted from the scattering experiments. To test this we performed integrations of equal-mass binaries in a Plummer model, starting the binaries as did Mikkola and Valtonen (1992). The Plummer model is better than the Jaffe model for this test because its large, flat core simplifies the 3-body prediction. Mikkola and Valtonen said that their N-body hardening rate agreed with the 3-body prediction, but we found a lower hardening rate (we checked the dependence on all our integration parameters); their rate might have been too large by chance, since the results are noisy with only 10^4 particles, the number that they used. To make a better comparison of the 3-body and N-body rates we performed a series of integrations like that of Mikkola and Valtonen but increasing the particle number and decreasing the BH masses by a factor of two each time, i.e. using $N/10^4 = 1, 2, 4, 8, 16$, together with $m_1 = m_2 = 1/100, 1/200, 1/400, 1/800, 1/1600$. The importance of loss-cone depletion goes down as m_1 is lowered with Nm_1 held fixed, because the mass of the binary goes down but the wandering amplitude does not. We found the N-body hardening rate to be about 0.5–0.7 as large as the 3-body prediction.

This change to the 3-body hardening rate is not important for estimates of merger times, given the much larger change that results from loss-cone depletion (we describe later how wandering changes the hardening rate when loss-cone depletion occurs). But the change to the ejection rate is important, because it means that before merging the binaries will eject about twice as much mass as we predicted in paper I. A question still to be answered is whether this is true for binaries with unequal masses.

5 The factors affecting the eccentricity evolution

We now study the factors affecting the eccentricity of a binary during the early stages of the evolution. We first consider binaries with equal or nearly-equal masses, whose early evolution can be predicted by the usual dynamical-friction formula, and then binaries with a large mass ratio, whose eccentricity may be influenced by resonant interactions with the stars.

5.1 Non-resonant friction

Chandrasekhar’s dynamical-friction formula can be used in most circumstances to predict the loss rates for energy and angular momentum as a BH binary forms at the center of a galaxy. The eccentricity is influenced by two competing factors. The velocity dependence

of the friction formula increases the frictional force at apocenter relative to that at pericenter if the BHs are moving fast, and therefore favors an increase in the eccentricity (Fukushige et al., 1992). The density gradient in the galaxy has the opposite effect if the density is higher at pericenter than at apocenter (Polnarev and Rees, 1994). Anisotropy is a further complication. Casertano et al. (1987) integrated the orbits of single massive particles in isotropic and radially anisotropic galaxy models using both Chandrasekhar’s formula and N-body methods, and found that anisotropy can counteract the density gradient and allow orbits to reach the center without their eccentricity decreasing. The eccentricity did not increase, however, unless the anisotropy was strong enough to make the galaxy susceptible to the radial-orbit instability.

Since Chandrasekhar’s formula is applicable only to the early stages of the binary evolution, the predictions that it makes for the eccentricity need to be checked by N-body experiments. Three previous studies have done this, all using a Plummer model to represent the galaxy. Makino et al. (1993) did experiments with 16,000 particles to study the formation and evolution of equal-mass binaries with BH masses ranging from 0.01 to 0.16. Their binaries sometimes formed with large eccentricities, but those experiments started with the BHs approaching the center on nearly radial orbits. Phinney and Villumsen (Phinney, 1994) did a similar experiment but started the BHs with a larger angular momentum (with $N = 4 \times 10^4$, $m_1 = 0.03$, $m_2 = 0.02$) and found that the eccentricity remained small. Mikkola and Valtonen (1992) also started the BHs with a large angular momentum and found a small initial eccentricity, although their experiment started with the binary nearly formed, and the noise level was high enough (with $N = 10^4$, $m_1 = m_2 = 0.01$) that the eccentricity bounced around in a random manner once the binary began to harden. The results from these studies were thus consistent with the predictions from Chandrasekhar’s formula, but were noisy and did not explore the effect of a density cusp or a radial anisotropy.

To improve upon this we performed experiments like those of Makino et al. (1993) but using a variety of galaxy models and initial orbits, and using a large number of particles to suppress the noise. For the galaxy models we used those of Plummer, Hernquist, and Jaffe, including for the Jaffe model both the isotropic model and a model with a constant radial anisotropy of $\beta = 1 - \sigma_t^2/\sigma_r^2 = 0.5$ (Cuddeford, 1991). This β value is small enough to suppress the radial-orbit instability (Merritt and Aguilar, 1985), which would be absent from our calculations in any case because we include only spherical basis functions in the expansion of the potential. The BHs had masses

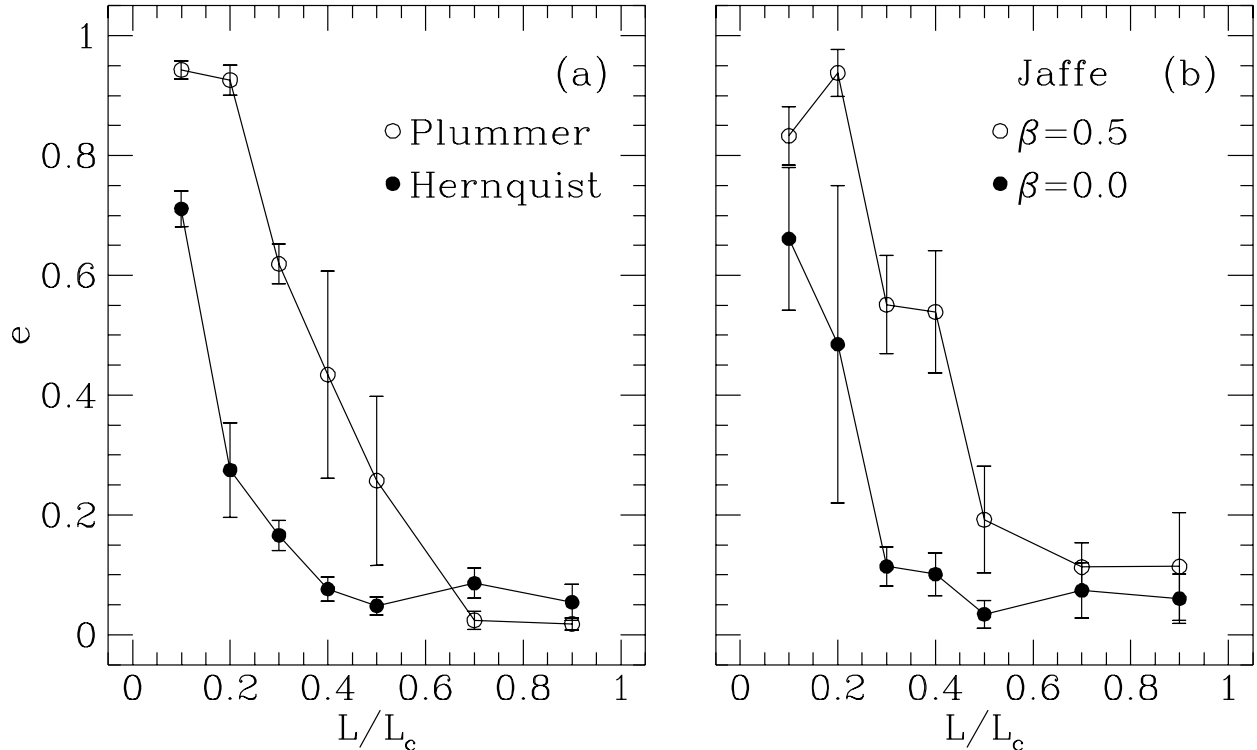


Figure 4: Eccentricity of an equal-mass binary when it first becomes hard at the center of a galaxy. The abscissa is the initial angular momentum of the BHS (at $r = 0.5$) in units of the angular momentum of a circular orbit of the same energy. The points and error bars show the mean eccentricity and the average deviation from the mean when the semimajor axis reaches $a = 0.004$, computed from 3–5 experiments with different orbital planes for the initial orbits. The isotropic ($\beta = 0$) Plummer and Hernquist models used $N = 10^5$ and $\lambda = 1$; the Jaffe models used $N = 2 \times 10^5$ and $\lambda = 0.5$.

$m_1 = m_2 = 0.01$ and were started symmetrically about the origin at (\vec{r}, \vec{v}) and $(-\vec{r}, -\vec{v})$, with $r = 0.5$ and with angular momenta equal to L/L_c times the angular momentum of a circular orbit of the same energy. The quantity that we measured is the eccentricity when the binary first becomes hard, i.e. when it reaches $a_h = Gm_2/4\sigma^2$.

The results in panel (a) of Figure 4 show that it is easier for a binary to form with a large eccentricity in the Plummer model than in the Hernquist model, in agreement with the prediction of Polnarev and Rees (1994) that a density cusp lowers the eccentricity. The isotropic Jaffe model is similar to the Hernquist model in this respect (the Jaffe-model results are noisier than the Hernquist-model results at small L/L_c , possibly because of the different velocity distributions in the two models). For the anisotropic Jaffe model the eccentricities are larger at small values of L/L_c but are still small if $L/L_c \gtrsim 0.6$, in agreement with the prediction of Casertano et al. (1987) that a radial anisotropy can allow an eccentric orbit to remain eccentric but cannot cause the eccentricity to

grow.

If the incoming BH orbits are distributed isotropically, the probability of an orbit of a given energy having an angular momentum less than L is $(L/L_c)^2$. The probability of a binary forming with a large eccentricity is therefore small. The formation of a BH binary after the merger of two galaxies will be more complicated than in the simple experiments considered here: the BHS will have clusters of bound stars, and the surrounding galaxies will be greatly disturbed. Barnes (1992) simulated the merger of disk galaxies (without BHS) and found that the final collision of the two bulges was often remarkably head-on, suggesting that small values of L/L_c might not be that improbable. But, as Barnes admits, the bulges in his galaxy models had unreasonably large core radii. If the bulges had been more concentrated their final collision might have had a larger L/L_c , for the same reason that the BHS in our calculations approach the center with a larger L/L_c when the galaxy has a density cusp. Thus, except for unusual cases in which a galaxy has a large, flat core or a strong radial anisotropy, we suspect that

most mergers of galaxies with central BHs will lead to binaries with small eccentricities.

5.2 Resonant friction

There is one circumstance in which dynamical friction can cause the eccentricity of a BH binary to increase even in the presence of a density cusp. Rauch and Tremaine (1996) described this in their discussion of resonant relaxation, and called the frictional force “resonant friction” because it results from resonant interactions between the stars and the smaller of the two BHs. Consider a BH of mass m_2 orbiting a larger BH of mass m_1 , with m_1 surrounded by a cluster of bound stars of total mass M_* , and assume that the stars have an anisotropic velocity distribution ($df/dL \neq 0$). If $m_1 \gg \max(m_2, M_*)$, the stars move in a potential that is nearly Keplerian and have orbits that are nearly closed. The frictional force on m_2 then cannot be described by the usual dynamical-friction formula. Rauch and Tremaine show that resonant interactions between m_2 and the stars increase $|dL/dt|$ by a factor of order $m_1/\max(m_2, M_*)$ but have no effect on $|dE/dt|$, and thus cause the eccentricity of the binary to change much faster than the semimajor axis; the sign is such that the eccentricity increases if $df/dL < 0$ (i.e. if the distribution is biased in favor of radial orbits) and decreases if $df/dL > 0$.

To determine the strength of the anisotropy required for resonant friction to be effective, we made five galaxy models having the same mass distribution but different anisotropies, each model containing a central BH of mass $m_1 = 0.1$ (see Fig. 5). We chose a large value for m_1 so that we could choose $m_2 \ll m_1$ and still have m_2 much more massive than the stars; one can think of our galaxy models in these experiments as representing the inner parts of real galaxies. Model D was made by growing m_1 slowly at the center of a γ model with $\gamma = 0$, which should lead to a final model with a cusp $\rho \sim r^{-2}$ and a central anisotropy $\beta \simeq -0.2$ (Quinlan et al., 1995); the central β value in the figure is slightly lower than the theoretical prediction because we removed some of the stars on radial orbits close to the BH. The other models were made by varying the cusp slope γ of the initial model and the growth time of the BH (short growth times lead to radial anisotropies, long growth times to tangential anisotropies), and sometimes by removing stars on orbits with low or high angular momenta after the BH growth was finished to get the desired mass and anisotropy profiles. The models were integrated for a while to check that they had reached equilibrium. Resonant friction should be important when a small mass m_2 sinks inside $r \lesssim 0.01$, where $M(r) \ll m_1$ and where the models have different anisotropies.

The orbits of small BHs were integrated in the five models starting at $r = 0.2$ and continuing until the binary semimajor axis reached $a \lesssim 0.001$. To reduce the cpu time, m_1 was fixed at the origin, which is what Rauch and Tremaine assumed. This assumption is not valid near the end of the integrations, when the binary is hard and the motion of m_1 would be important, but it does not affect the eccentricity much when m_2 first enters the region $r \lesssim 0.01$; we checked that by repeating a few of the integrations without fixing m_1 . Figure 6 shows the eccentricity evolution for m_2 values 0.001, 0.003, and 0.01. The eccentricity and semimajor axis in this figure are generalized orbital elements that agree with the Kepler elements when the BHs are close and give useful information when they are not close (the semimajor axis then gives an estimate of the distance between the BHs). Since resonant friction should increase the eccentricity if $\beta > 0$ and decrease it if $\beta < 0$, the initial eccentricities were chosen to be small for the radial models ($\beta > 0$) and large for the tangential models ($\beta < 0$).

Consider first the results in panel (a) from the integrations with $m_2 = 0.001$. The influence of anisotropy on the eccentricity is clear: in models A and B, with radial anisotropies, the eccentricity grows larger, whereas in models D and E, with tangential anisotropies, it grows smaller. In models A and E the eccentricity changes much faster than the semimajor axis when $1/a \simeq 100$, as Rauch and Tremaine predicted. The evidence from the integrations with larger m_2 values is not as clear. The eccentricity still grows in model A when $m_2 = 0.003$, suggesting that resonant friction still operates, but the growth is not as fast as with $m_2 = 0.001$. When $m_2 = 0.01$ the eccentricity goes down in all the models, and the rate of change is low enough to be explained by ordinary, non-resonant friction. This m_2 value perturbs the resonances responsible for resonant friction.

Thus resonant friction can cause a rapid growth in the eccentricity of a BH binary, but only if two conditions are satisfied: first, m_2 must be at least 30 times smaller than m_1 (this was implicit in the formulas of Rauch and Tremaine); second, and more troublesome, the cluster of stars bound to m_1 must have a strong radial anisotropy, say $\beta > 0.5$. There is no reason to expect an anisotropy like that around a massive BH. The only existing models for the formation of BHs in galaxies that make definite predictions for the anisotropy—the adiabatic-growth model (Young, 1980; Goodman and Binney, 1984; Quinlan et al., 1995), and the binary-merger model studied here—predict a tangential anisotropy. Any model in which the BH grows by consuming stars on radial orbits is likely to favor a tangential anisotropy. Some formation models may allow a radial anisotropy (e.g.,

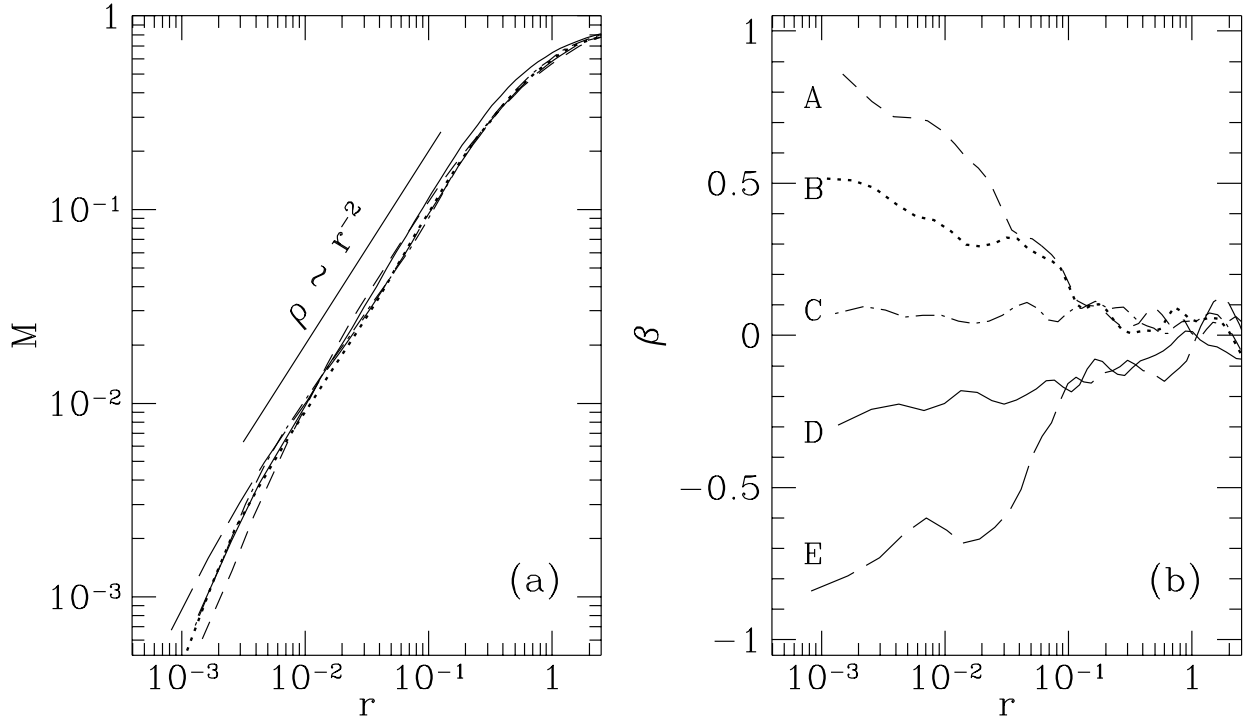


Figure 5: Anisotropy $\beta = 1 - \sigma_t^2/\sigma_r^2$ and enclosed stellar mass M for the inner parts of five models used to study resonant friction. Each model has $N = 50K$ particles with a mass exponent $\lambda = 0.75$, and a central BH of mass $m_1 = 0.1$ with a BH-star softening length of 0.00025.

models that involve a sudden collapse at the center, with the BH and the stars forming simultaneously), but they have not been studied and are unlikely to predict an anisotropy as strong as $\beta > 0.5$. There are two galaxies for which we have estimates of the anisotropy around the central BH. If the BH mass estimate of Harms et al. (1994) for M87 is correct, then the best fit to the stellar velocity distribution has a tangential anisotropy, although the error bars are large enough to allow a slight radial anisotropy (Dressler and Richstone, 1990; Merritt and Oh, 1996). For M32 also the best fit to the velocity distribution around the central BH has a tangential anisotropy (van der Marel et al., 1997).

Although we do not believe that resonant friction will be important for the eccentricity evolution of BH binaries, the possibility of this is nevertheless interesting: it shows the danger of relying on the simple dynamical-friction formula. Resonant friction may be more important for binaries in galaxies with disks, where it will affect the inclination as well as the eccentricity.

6 The response of the galaxy

The response of a galaxy to the hardening of a BH binary may explain why large elliptical galaxies have weaker density cusps than smaller galaxies. Figures 1 and 3 showed some results for the core expansion and mass ejection caused by a binary at the center of a Jaffe model. Here we examine the change in the density profile for a range of binary masses, and also the kinematical signature that the binary leaves in the velocity distribution. We again use a Jaffe model to represent the galaxy; the results will apply with some changes to models with other gamma values.

We integrated binaries with five masses ($m_1 = m_2 = 0.04, 0.02, 0.01, 0.005, \text{ and } 0.0025$), starting them as we did for the integration in Figure 1. The galaxy model had 10^5 particles with a mass exponent $\lambda = 0.75$. To study the change in the galaxy we kept frequent records of the radii containing fixed fractions of the total mass, like the radii in panel (c) of Figure 1 but more of them, and also of the sums of mv_r^2 and mv_t^2 for the stars inside those radii. By differentiating the mass fractions and velocity sums with respect to radius, after first smoothing their time dependence, we were able to recover the density and the radial and tangential dispersions at any time during

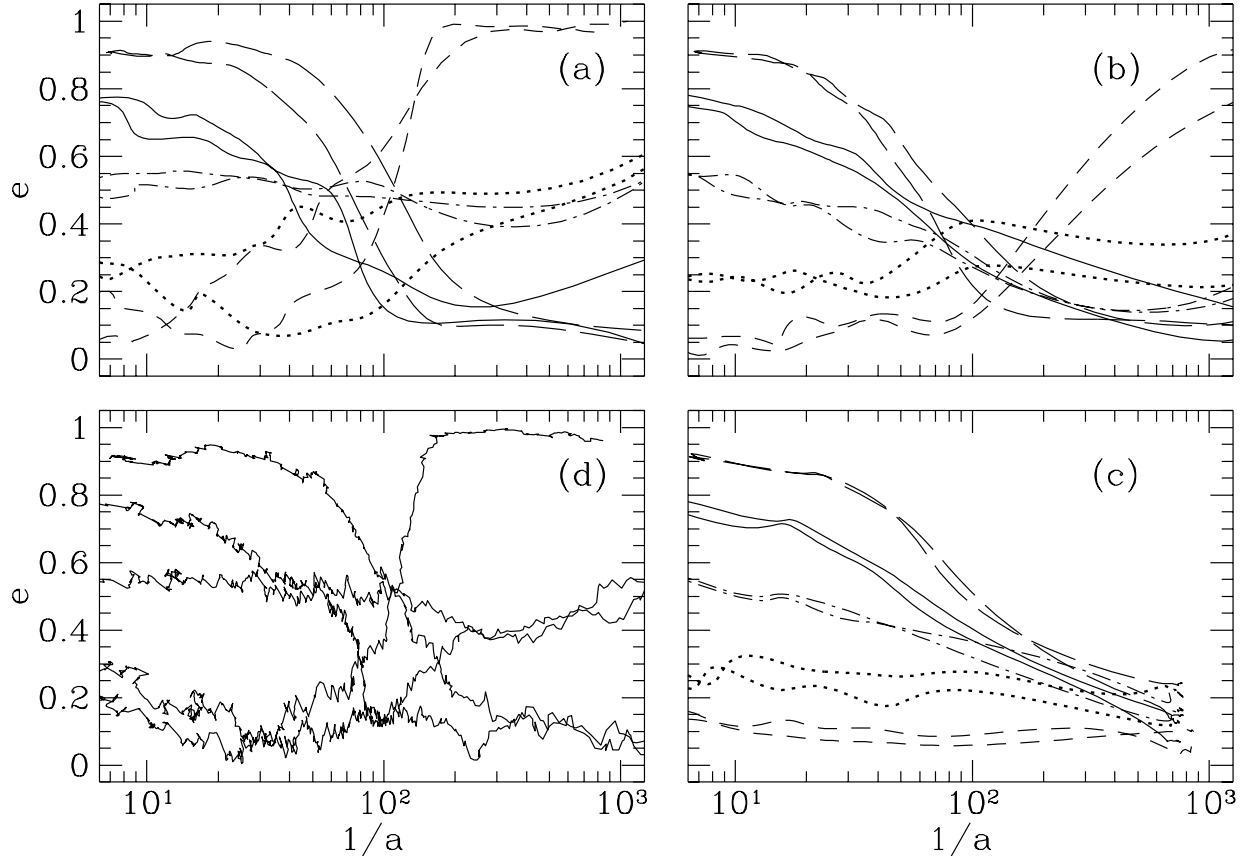


Figure 6: Eccentricity versus semimajor axis for BHs of mass $m_2 = 0.001$ (a), 0.003 (b), and 0.01 (c) orbiting in the five models of Figure 5 (the different line types correspond to those used in Fig 5). The two lines for each model and m_2 value are from integrations in which m_2 was started in a clockwise and counter-clockwise sense. Panel (d) shows five of the lines from panel (a) before they were smoothed. The orbital elements are defined (for this figure only) by $1/a = -2E/m_1$ and $e = \sqrt{1 - L^2/L_c^2}$, with E and L the energy and angular momentum of m_2 and with the potential of the galaxy set to zero at $r = 0.2$ for the calculation of E .

the integrations. We use this data in Figure 7 to plot the densities and dispersions when the five binaries reached $V_{\text{bin}} = 4$, the highest velocity reached by the binary with $m_1 = 0.04$ (we stopped the integration then because it was becoming slow). The binaries with smaller masses reached higher velocities, but to study the dependence on the binary mass it is best to compare the galaxies at the same V_{bin} .

The density profiles in panel (a) show that a binary can eliminate a density cusp. Although the profile for the smallest binary has a mild cusp, the others have densities that are flat or, in some cases, decreasing towards the center; they would probably all decrease if we could plot them closer to the center (this was predicted by Begelman et al. 1980). The mass ejected from the central region is $M_{\text{ej}}/M_{12} = 1.2\text{--}1.5$, as we reported in Figure 3, with no systematic dependence of M_{ej}/M_{12} on the binary mass. Because the Jaffe model has a mass that, near the center, in-

creases linearly with radius, the core radius at a fixed V_{bin} increases linearly with the binary mass; for other gamma models the dependence would be nonlinear. The M_{ej}/M_{12} values computed here are larger than we predicted in paper I, partly because some mass gets displaced from the center in the N-body experiments before the binaries form and partly because, as we discussed in Section 4, the ejection rates once the binaries form in the N-body experiments (and, we believe, in real galaxies) are higher than we predicted in paper I. As the binaries continue hardening, more mass will be ejected and the core radii will grow. For example, Figure 3 shows the density profile for the binary with $m_1 = 0.01$ at $V_{\text{bin}} = 6.8$: the central density is less than half of its value at $V_{\text{bin}} = 4$, and the core radius is nearly twice as large. The final profile will depend on how far the binary has to harden before gravitational radiation becomes important. Massive BH binaries in typical galaxy cores have to shrink by

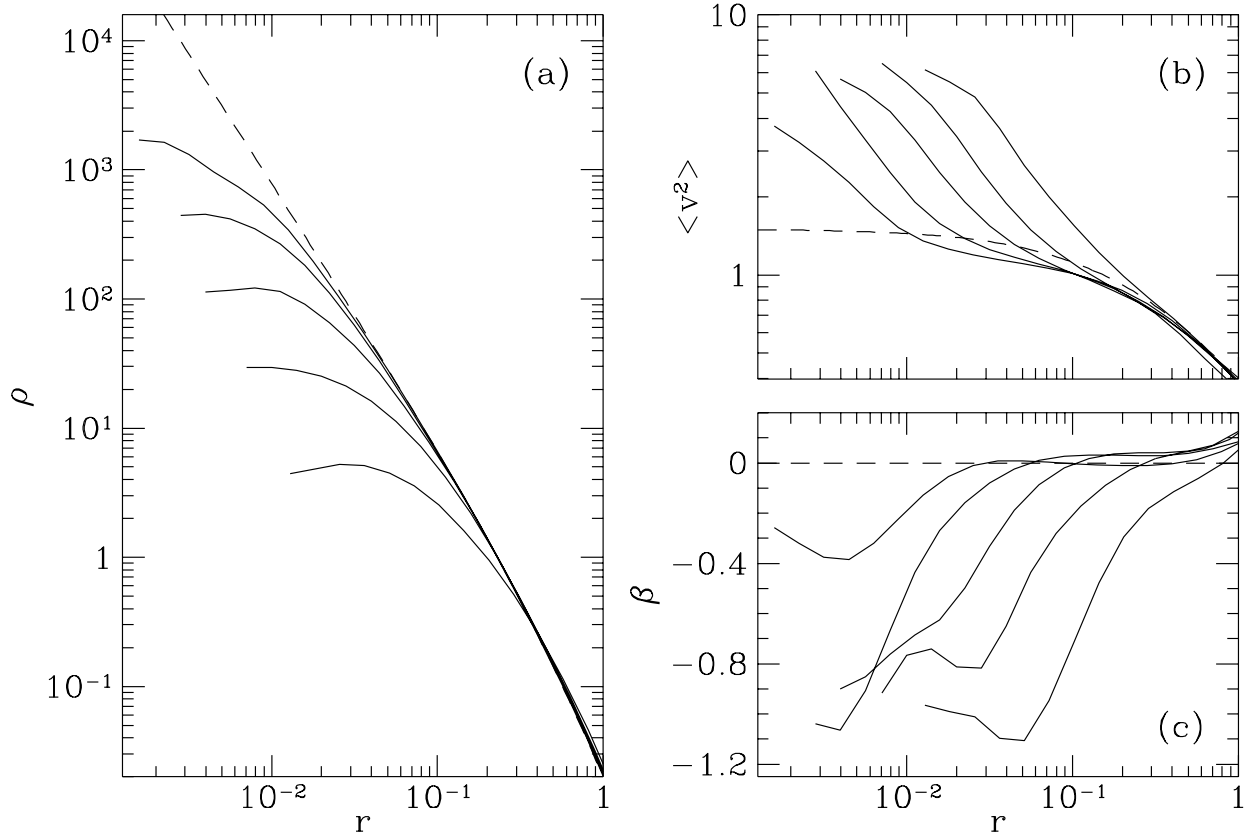


Figure 7: Response of a Jaffe model to the hardening of a BH binary. The dashed lines show the initial (a) density, (b) 3D velocity dispersion, and (c) anisotropy. The solid lines show these quantities when the binary reaches $V_{\text{bin}} = 4$, with the binary started as in Fig. 1, and with the five lines for BH masses $m_1 = m_2 = 0.04$ (rightmost line), 0.02, 0.01, 0.005, and 0.0025 (leftmost line).

a factor of 10–50 beyond the point at which they become hard, with the factor varying with the BH masses as $M_{12}^{2/5}$ for an equal-mass binary. The binaries in Figure 7 shrank about a factor of 4 beyond the point at which they became hard. In a typical galaxy they would have to shrink another factor of 3–12, causing V_{bin} to rise by a factor of 1.7–3.5 and, using Figure 3 as a guide, adding 0.4–0.8 to the value of M_{ej}/M_{12} .

The kinematical response of the galaxy is shown in panels (b) and (c). The velocity dispersions rise towards the center, approximately (but not exactly) as $v^2 \sim 1/r$. Mass estimates derived from these dispersions will underestimate the central masses if the anisotropies are not taken into account. The models all develop strong tangential anisotropies, because the stars on radial orbits are the ones that get ejected. Four of the five lines in panel (c) show $\beta \simeq -1$ near the center, although we see no reason why that value should be preferred. The central anisotropy is difficult to measure (the leftmost parts of our lines are affected by noise); we expect that β would fall below -1 if we

could measure it closer to the binary. This is a much stronger anisotropy than is predicted by models like the adiabatic-growth model for the formation of massive black holes. The adiabatic growth of a BH in an initially isotropic galaxy leads to a final anisotropy of at most $\beta = -0.3$ (Quinlan et al., 1995)

Our mass-ejection results support the suggestion of Ebisuzaki et al. (1991) and Faber et al. (1996) that BH binaries can explain the weak density cusps in large elliptical galaxies. If these galaxies contain massive BHs, and if they have formed through mergers of smaller galaxies also containing massive BHs, the binaries that result will clear out the central region. A real galaxy merger will of course be more complicated than the idealized experiments considered here. In most cases a binary will result when a small satellite galaxy sinks into a large galaxy containing a massive BH. The scattering experiments from paper I suggested that more mass gets ejected if a massive BH merges with a number of small BHs than if it merges with one large BH (with the same total mass), although each small BH

may counteract the mass ejection to some extent by bringing fresh stars and gas to the center. The general result from our experiments should remain true: the density cusp in a merged galaxy will be weaker if the merger leads to a BH binary. And with this result we can make a testable prediction: if this is the explanation for the weak density cusps in large galaxies, the central velocity distributions in those galaxies should have strong tangential anisotropies. As we mentioned in Section 5, there is evidence that the galaxy M87 passes this test.

7 The binary merger time in real galaxies

The answer to many questions involving massive BH binaries depends on the binary merger time. A big uncertainty in computing this has been loss-cone depletion. Although the loss cone can be replenished if the potential is nonspherical, and the binary merger can be helped by gas accretion onto the BHs, for many galaxies these perturbations will not be enough. We therefore consider whether a binary can merge through purely stellar dynamical processes in a spherical galaxy. We believe that the answer is often yes, thanks to the wandering of the binary from the galaxy center.

Previous discussions of the loss-cone problem have mostly assumed that the central object (a single BH or a binary) remains fixed at $r = 0$. The rate at which stars accrete onto or interact with the object once the loss cone becomes depleted is then given by an expression of the form (e.g., Shapiro, 1985)

$$\frac{dM}{dt} \sim \frac{\rho(r_{\text{crit}})r_{\text{crit}}^3}{t_r(r_{\text{crit}})\ln(r_{\text{crit}}/r_{\text{D}})}, \quad (9)$$

where r_{D} is the destruction or interaction radius, which we take to be the binary semimajor axis, and r_{crit} is the radius at which the loss-cone angle θ_{lc} equals the rms deflection suffered by stars through two-body relaxation in one dynamical time. For BH binaries in typical galaxies, r_{crit} is larger than GM_{12}/σ^2 , and the relaxation time at r_{crit} is much longer than the age of the galaxy. The hardening rate implied by equation (9) is then too low to allow most binaries to merge.

Valtonen (1996) used the galaxy M87 to illustrate how difficult it is for a central binary to merge when the relaxation time is long. He considered an equal-mass binary with $M_{12} = 3 \times 10^9 M_{\odot}$ and a separation $a = 0.6$ pc, at which the merger time from gravitational radiation is 10^{10} yr, and at which the total mass in stars that can approach within a of the center—assuming that the loss cone is not depleted—is only

1/200 of the mass of the binary. For the binary to shrink by a factor of e , the loss cone would have to be refilled about 200 times. The problem is worse for smaller BHs because they have to shrink more before radiation becomes important. For $M_{12} = 3 \times 10^6 M_{\odot}$ the factor of 200 in Valtonen’s example gets replaced by 7800. Valtonen concluded that, for nearly the whole range of parameters of interest, BH binaries in galaxies are incapable of merging.

Wandering changes this conclusion. We refer here not to the small correction to the hardening rate that we discussed in Section 4, but to a larger correction that occurs when the loss cone becomes depleted. A simple equipartition estimate predicts that a particle of mass M_{12} (a single BH or a binary) in a homogeneous core of smaller particles of mass m will have a maximum wandering amplitude

$$r_{\text{w}} \simeq r_{\text{c}} \left(\frac{m}{M_{12}} \right)^{1/2}. \quad (10)$$

Young (1977) argued that this amplitude is sometimes large enough to affect the growth of BHs in the centers of galaxies, but most subsequent work has either ignored wandering or has dismissed it as unimportant. For BH binaries we believe that wandering is even more important than Young suggested, because the prediction (10) underestimates the wandering amplitude of a BH binary. The prediction is applicable to a massive particle in a homogeneous core, but a BH binary ejects stars from the center of the core, reducing the restoring force that keeps it at the center, and the superelastic encounters between the binary and the stars invalidate the equipartition assumption on which the prediction is based. Consider the integration that we used earlier as an example. The core radius in Figure 3 is $r_{\text{c}} \simeq 0.04$ (derived by fitting a King-model core to the final density), and the mass ratio is $m/M_{12} \lesssim 10^{-5}/0.02$ (this would be an equality if the stars had equal masses), so the prediction (10) gives $r_{\text{w}} \lesssim 0.0009$. But the maximum wandering amplitude shown in Figure 1 is more than five times as large. And, as we mentioned in Section 3, the amplitude remained the same when we raised N from 10^5 to 2×10^5 , making the discrepancy with the prediction even larger.

We suspect that in many galaxies it is the wandering of the binary, and not diffusion of stars into the loss cone, that determines the hardening rate once the loss cone gets depleted. In our Jaffe-model integration, for example, the hardening rate did not increase when we added non-spherical terms to the potential by changing l_{max} from 0 to 2, even though this change made the potential noisier, somewhat like the way that two-body relaxation does, and allowed more stars to

reach the center. The change did increase the hardening rate when we applied a constraint force to fix the binary at the center of the galaxy.

Wandering will not be enough to allow all BH binaries to merge. It allows a binary to continue hardening beyond the point at which it would stop without wandering, but the hardening continues at a reduced rate. As a rough guide, we can say from our integrations that once a binary ejects the stars from its immediate vicinity and creates a core, it hardens at a rate that is about 10–50 times slower than the rate we predicted in paper I ignoring loss-cone depletion. Whether this will be fast enough to allow a merger depends on the particular galaxy under study. Gas and nonspherical perturbations will help if they are present.

These conclusions have been derived for equal-mass binaries. The most likely formation scenario for a massive BH binary is for a small satellite galaxy containing a central BH to sink into a larger galaxy with a larger BH. The bottleneck in this case may be the time required for the small BH to reach the center. N-body experiments by Balcels and Quinn (1989, 1990) show that small, dense satellites can easily sink into the center of large elliptical galaxies, but Weinberg’s (1997) perturbation calculations suggest that this is not always the case. If the satellite galaxy surrounding the small BH gets disrupted, the BH will take longer to reach the center. Neither Weinberg nor Balcels and Quinn included BHs in their models; some preliminary experiments with BHs have been done by Governato et al. (1994). More work on this is needed, since the predicted merger rate for the gravitational-wave detector LISA is much larger if small BHs can participate in the mergers (Haehnelt, 1994).

Acknowledgements

We thank Sandra Faber, Jeremiah Ostriker, Martin Rees, and Scott Tremaine for helpful discussions while this work was in progress. We are especially grateful to Sverre Aarseth for helping us use his N-body integration routines in our hybrid program. Financial support was received at UCSC from the NSF under grant ASC 93-18185 and the Presidential Faculty Fellows Program, and at Rutgers from NSF grant AST 93-18617 and NASA Theory grant NAG 5-2803.

A The hybrid N-body program

We describe here some technical details of our hybrid N-body program. We assume that the star cluster contains two BHs, but the program can work with any number of BHs. Our notation follows that of Aarseth (1994) and Hernquist and Ostriker (1992).

A.1 The integrator

The program uses different integrators for the BHs and the stars. The stars are integrated with the NBODY1 integrator. The stepsizes for the stars vary continuously and are updated after each step by a function involving the force and the first three time derivatives of the force, multiplied by the square root of an accuracy parameter η . We used $\eta = 0.005$ – 0.01 , smaller than the value that Aarseth recommends ($\eta = 0.02$ – 0.03), so that we could integrate close encounters accurately with a small softening length. The BHs are integrated with the NBODY2 integrator, which uses the Ahmad-Cohen neighbor scheme. The BHs have two stepsizes, δt_i and δt_r , determined by two accuracy parameters, $\eta_i = \eta$ and $\eta_r = 2\eta_i$. The BHs are moved and the irregular force from nearby stars (the neighbors) is updated on the smaller stepsize δt_i ; the regular force from the remaining stars is updated on the larger stepsize δt_r and is predicted between those times from its known time derivatives. The number of neighbors for each BH is set to approximately $(N/4)^{3/4}$, the scaling recommended by Makino and Hut (1988); the program forces each BH to be in the neighbor list of the other BH at all times. When N is large, δt_i is usually much smaller than δt_r . The neighbor scheme improved the efficiency of our integrations by at least a factor of ten.

The program checks periodically to see if the BHs are close enough for their motion to be regularized. If they are, the BHs are replaced by a center-of-mass particle and a set of KS coordinates describing their relative motion. Our criterion for “close enough” is that each BH is the closest neighbor of the other BH, that the force on each BH from the other BH is five times larger than the force from the stars, and that the neighbor list for the center-of-mass particle is large enough to contain the perturbers for the KS coordinates, which means the stars that exert a dimensionless perturbation exceeding a value γ_{\min} . The KS equations of motion are integrated with the Hermite integrator from the NBODY6 program; the center-of-mass motion is integrated with the NBODY2 integrator as is the motion of single BHs, except that the forces between the center of mass and nearby stars (those within a distance λa) are computed by resolving the binary into its two BHs. We used $\lambda = 1000$, probably much larger than was necessary (Aarseth recommends $\lambda = 70$). The KS stepsize is chosen so that the number of steps per unperturbed period is $2\pi/\eta_u$, with η_u the KS accuracy parameter (Aarseth recommends $\eta_u \lesssim 0.1$; we used 0.07). If the binary has no perturbers, the Keplerian motion is integrated exactly. Even with perturbers, regularization allows close binaries to be integrated efficiently regardless of

their eccentricity, with no softening needed for the BH-BH interaction.

The large difference between the masses of the BHs and the stars in our experiments caused some difficulties with the standard KS integration procedures. When we used the value for γ_{\min} that Aarseth recommends (10^{-6}) the stepsize for the center-of-mass particle was sometimes much smaller than the stepsize for the KS coordinates, because a small star near the massive binary does not get included in the list of KS perturbers if its dimensionless perturbation is less than γ_{\min} , but it does get included in the center-of-mass neighbor list and it affects the center-of-mass stepsize. Large errors can result if there are many such stars. To improve the accuracy we reduced γ_{\min} to 10^{-7} , and we introduced a parameter $\Gamma = 50$ so that stars within a distance Γa of the binary are included in the KS perturber list whatever the size of their perturbation. Although these precautions slowed our integrations somewhat, the integration of close binaries still went several times faster when regularization was used.

Because the program regularizes only the motion of the BH binary, and not the motion of stars approaching the binary, the interactions between the BHs and the stars have to be softened; otherwise some stars would be given tiny stepsizes when they encounter the BHs. We chose the softening length so that the softening velocity (eq. 6) was at least 2–3 times as large as the velocity of the binary at the end of the integration; three-body scattering experiments showed that a softening length of that size does not affect the average energy transfer. Even with softening we sometimes had trouble with stars that got captured into tightly bound orbits around the BHs. We therefore merged stars with the BHs if they were captured into orbits with semimajor axes less than twice the softening length. The number of stars merged in this way was small: the growth of the BH masses was at most 0.2%.

A.2 The expansion of the potential

The coefficients A_{nlm} for the potential expansion are updated at fixed time intervals Δt , after the coordinates of the stars are first predicted to a common time. We used the basis functions of Hernquist and Ostriker (the lowest-order member of the set is the Hernquist potential), but adjusted the scale length d for each initial model to customize the fit (Hernquist and Ostriker assume that $d = 1$). We found it necessary to soften the basis functions by replacing the radius r of a particle by $(r^2 + h^2)^{1/2}$, with $h \simeq 10^{-4}$, for otherwise our use of both a mass spectrum and an integrator with individual stepsizes sometimes caused

stars to get trapped in orbits with tiny stepsizes at the center of the galaxy. In most of our integrations we used a spherical basis ($l_{\max} = 0$), with the number of functions in the range $10 \leq n_{\max} \leq 20$, depending on the initial model (the Jaffe model required largest n_{\max}). With a spherical basis the expansion assumes that the center of mass of the galaxy is fixed at the origin, an assumption that has been shown to artificially accelerate the orbital decay of satellite galaxies in the sinking-satellite problem (White, 1983), although only when the satellite is far from the center of the primary galaxy (Quinn and Goodman, 1996). The assumption should not affect the evolution rate in our BH-binary experiments, because the BHs start close to the center and often symmetrically about the center, making the dipole distortion of the galaxy small. When we used a spherical basis the cpu time spent computing the expansion functions was at most half of the total cpu time; most of the time was spent computing the forces between the BHs and the stars.

The NBODY1 integrator needs the forces and the first three time derivatives of the forces acting on the stars at the start of an integration. This initialization is cumbersome when the expansion method is used. In principle the derivatives could be computed analytically from the expansion functions, but in practice we used the known derivatives for the initial galaxy model, or used numerical interpolation to approximate the derivatives. This would have been simpler if we had used the Hermite integrator for the stars, as that requires only the first time derivative (Makino 1991).

A.3 Tests and possible improvements

We ran a number of tests to check the integrators and the potential expansion. We first fixed the expansion coefficients and checked that the conservation of energy improved in the manner expected for Aarseth’s fourth-order integrators when we reduced the accuracy parameters η and η_u . We also checked that the evolution of a hard binary was independent of which integrator we used for the BHs (NBODY1, NBODY2, or NBODY6), provided that the accuracy parameters were small (the required cpu time, of course, depends on the integrator). To test the potential expansion we checked that the program could maintain equilibrium γ models without BHs for radii $r \gtrsim 10^{-2}$ (the minimum radius depends on γ and n_{\max}). We also repeated some of our BH-binary experiments using the basis functions of Clutton-Brock (1973) instead of those of Hernquist and Ostriker, to check that the two gave the same result when n_{\max} was large.

One test did reveal an important limitation of our program. We ran some cold-collapse experiments

(starting a galaxy with the stars at rest, with no BHs) to check that the SCFBDY and SCF programs gave the same result for the virial ratio versus time. They did, but only if we used a stepsize Δt with SCFBDY considerably smaller than the stepsize required with SCF. The reason is that with SCFBDY the updating of the expansion coefficients is not time reversible. The energy error after a fixed time therefore varies linearly with Δt with SCFBDY, and not quadratically as it does with SCF. This did not matter for our work, because the change in the potential was slow and we were able to choose Δt small enough to make the errors small, but it would matter for a problem with a rapidly changing potential.

Some improvements to the program may be possible. The particles could be given block stepsizes to make the program run faster on vector computers, although the vectorization will always be hindered by the complicated integration algorithm. The need to soften the BH-star interactions could be removed by more-sophisticated regularization, although this would be difficult when many stars interact with the BHs simultaneously. And the limitations of the potential expansion—such as the linear dependence of the error on Δt , and the difficulty of resolving small stellar clumps away from the center—could be reduced by updating the contribution to the expansion coefficients from the inner part of the galaxy more frequently than the contribution from the outer part, or by using the direct-summation method for the inner part and an expansion method only for the outer part, although either of these changes would increase the program complexity, and using the direct-summation method would increase the cpu time. We did not try any of these ideas.

References

- Aarseth, S.J., 1994, Direct methods for N-body simulations, in *Galactic Dynamics and N-Body Simulations*, edited by Contopoulos, G., Spyrou, N.K., & Vlahos, L., pp. 277–312 (Springer-Verlag).
- Balcells, M. & Quinn, P.J., 1989, Merger origin for the velocity and density substructure in elliptical galaxies, *Ap&SS*, 156, 133–140.
- Balcells, M. & Quinn, P.J., 1990, The formation of counterrotating cores in elliptical galaxies, *ApJ*, 361, 381–393.
- Barnes, J.E., 1992, Transformations of galaxies. I. Mergers of equal-mass stellar disks, *ApJ*, 393, 484–507.
- Begelman, M.C., Blandford, R.D., & Rees, M.J., 1980, Massive black hole binaries in active galactic nuclei, *Nature*, 287, 307–309.
- Bender, P., Ciufolini, I., Danzmann, K., et al., 1995, LISA: Pre-Phase A Report, Technical Report MPQ 208, Max-Planck Institut für Quantenoptik, Garching.
- Byun, Y.-I., Grillmair, C.J., Faber, S.M., et al., 1996, The centers of early-type galaxies with HST. II. Empirical models and structural parameters, *AJ*, 111, 1889–1900.
- Casertano, S., Phinney, E.S. & Villumsen, J.V., 1987, Dynamical friction and orbit circularization, in *Structure and Dynamics of Elliptical Galaxies*, edited by de Zeeuw, T., pp. 475–476, D. Reidel.
- Clutton-Brock, M., 1973, The gravitational field of three-dimensional galaxies, *Ap&SS*, 23, 55–69.
- Crane, P., Stiavelli, M., King, I.R., et al., 1993, High resolution imaging of galaxy cores, *AJ*, 106, 1371–1393.
- Cuddeford, P., 1991, An analytic inversion for anisotropic spherical galaxies, *MNRAS*, 253, 414–426.
- Dehnen, W., 1993, A family of potential-density pairs for spherical galaxies and bulges, *MNRAS*, 265, 250–256.
- Dressler, A. & Richstone, D.O., 1990, New measurements of stellar kinematics in the core of M87, *ApJ*, 348, 120–126.
- Ebisuzaki, T., Makino, J. & Okumura, S.K., 1991, Merging of two galaxies with central black holes, *Nature*, 354, 212–214.
- Faber, S.M., Tremaine, S., Ajhar, E.A., et al., 1996, The centers of early-type galaxies with HST. IV. Central parameter relations, *Astron. J.*, submitted (astro-ph/9610055).
- Ferrarese, L., van den Bosch, F.C., Ford, H.C., Jaffe, W. & O’Connell, R.W., 1994, Hubble Space Telescope photometry of the central regions of Virgo cluster elliptical galaxies. III. Brightness profiles, *AJ*, 108, 1598–609.
- Forbes, D.A., Franx, M. & Illingworth, G.D., 1995, Ellipticals with kinematically distinct cores: WFPC1 imaging of nearby ellipticals, *AJ*, 109, 1988–2002.
- Fukushige, T., Ebisuzaki, T. & Makino, J., 1992, Rapid orbital decay of a black hole binary in merging galaxies, *PASJ*, 44, 281–289.
- Gaskell, C.M., 1996, Supermassive binaries and extragalactic jets, in *Jets from Stars and Galactic Nuclei*, edited by Kundt, W., pp. 165–195 (Springer-Verlag).
- Goodman, J. & Binney, J., 1984, Adding a point mass to a spherical stellar system, *MNRAS*, 207, 511–515.
- Governato, F., Colpi, M., & Maraschi, L., 1994, The fate of central black holes in merging galaxies, *MNRAS*, 271, 317–322.
- Haehnelt, M.G., 1994, Low-frequency gravitational waves from supermassive black holes, *MNRAS*, 269, 199–208.
- Harms, R.J., Ford, H.C., Tsvetanov, Z.I., et al., 1994, HST FOS spectroscopy of M87: Evidence for a disk of ionized gas around a massive black hole, *ApJ Lett*, 435, L35–L38.
- Hernquist, L., 1990, An analytical model for spherical galaxies and bulges, *ApJ*, 356, 359–364.
- Hernquist, L. & Ostriker, J.P., 1992, A self-consistent field method for galactic dynamics, *ApJ*, 386, 375–397.
- Hut, P. & Rees, M.J., 1992, Constraints on massive black holes as dark matter candidates, *MNRAS*, 259, 27p–30p.
- Jaffe, W., 1983, A simple model for the distribution of

- light in spherical galaxies, *MNRAS*, 202, 995–999.
- Kormendy, J. & Richstone, D., 1995, Inward bound - the search for supermassive black holes in galactic nuclei, *Ann. Rev. Astron. Astrophys.*, 33, 581–624.
- Lauer, T.R., Ajhar, E.A., Byun, Y.-I., et al., 1995, The centers of early-type galaxies with HST. I. An observational survey, *AJ*, 110, 2622–2654.
- Lauer, T.R., Faber, S.M., Growth, E.J., et al., 1993, Planetary Camera observations of the double nucleus of M31, *AJ*, 106, 1436–1447.
- Makino, J., 1991, Optimal order and time-step criterion for Aarseth-type N-body integrators, *ApJ*, 369, 200–212.
- Makino, J., 1997, Merging of galaxies with central black holes. II. Evolution of the black hole binary and the structure of the core, *ApJ*, 478, 58–65.
- Makino, J. & Ebisuzaki, T., 1994, Triple black holes in the cores of galaxies, *ApJ*, 436, 607–610.
- Makino, J. & Ebisuzaki, T., 1996, Merging of galaxies with central black holes. I. Hierarchical mergings of equal-mass galaxies, *ApJ*, 465, 527–533.
- Makino, J., Fukushige, T., Okumura, S.K. & Ebisuzaki, T., 1993, The evolution of massive black-hole binaries in merging galaxies. I. Evolution of a binary in a spherical galaxy, *PASJ*, 45, 303–310.
- Makino, J. & Hut, P., 1988, Performance analysis of direct N-body calculations, *ApJ Suppl. Ser.*, 68, 833–856.
- Merritt, D. & Aguilar, L.A., 1985, A numerical study of the stability of spherical galaxies, *MNRAS*, 217, 787–804.
- Merritt, D. & Oh, S.P., 1997, The stellar dynamics of M87, *Astron. J.*, 113, 1279–1285.
- Mikkola, S. & Valtonen, M.J., 1992, Evolution of binaries in the field of light particles and the problem of two black holes, *MNRAS*, 259, 115–120.
- Phinney, E.S., 1994, Mass-transfer induced activity in galaxies: an introduction, in *Mass-Transfer Induced Activity in Galaxies*, edited by Shlosman, I., pp. 1–22, Cambridge University Press.
- Polnarev, A.G. & Rees, M.J., 1994, Binary black hole in a dense star cluster, *Astron. Astrophys.*, 283, 301–312.
- Quinlan, G.D., 1996, The dynamical evolution of massive black hole binaries. I. Hardening in a fixed stellar background, *NewA*, 1, 35–56.
- Quinlan, G.D., Hernquist, L., & Sigurdsson, S., 1995, Models of galaxies with central black holes: adiabatic growth in spherical galaxies, *ApJ*, 440, 554–564.
- Quinn, P.J. & Goodman, J., 1986, Sinking satellites of spiral systems, *ApJ*, 309, 472–495.
- Rajagopal, M. & Romani, R.W., 1995, Ultra-low frequency gravitational radiation from massive black hole binaries, *ApJ*, 446, 543–549.
- Rauch, K.P. & Tremaine, S., 1996, Resonant relaxation in stellar systems, *NewA*, 1, 149–170.
- Roos, N., 1981, Galaxy mergers and active galactic nuclei, *Astron. Astrophys.*, 104, 218–228.
- Roos, N., 1988, Jet precession in active galaxies, *ApJ*, 334, 95–103.
- Roos, N., Kaastra, J.S. & Hummel, C.A., 1993, A massive binary black hole in 1928+738?, *ApJ*, 409, 130–133.
- Saslaw, W.C., Valtonen, M.J. & Aarseth, S., 1974, The gravitational slingshot and the structure of extragalactic radio sources, *ApJ*, 190, 253–270.
- Shapiro, S.L., 1985, Monte Carlo simulations of the 2+1 dimensional Fokker-Planck equation: spherical star clusters containing massive, central black holes, in *Dynamics of Star Clusters*, edited by Goodman, J. & Hut, P., pp. 373–413 (Reidel).
- Sigurdsson, S., Hernquist, L. & Quinlan, G.D., 1995, Models of galaxies with central black holes: simulation methods, *ApJ*, 446, 75–85.
- Tremaine, S., 1995, An eccentric-disk model for the nucleus of M31, *AJ*, 110, 628–633.
- Tremaine, S., Richstone, D., Byun, Y.-I., et al., 1994, A family of models for spherical stellar systems, *AJ*, 107, 634–644.
- Valtonen, M.J., 1996, Are supermassive black holes confined to galactic nuclei?, *Comm. Astrophys.*, 18, 191–206.
- Valtonen, M.J., Mikkola, S., Heinamaki, P. & Valtonen, H., 1994, Slingshot ejections from clusters of three and four black holes, *ApJ Suppl. Ser.*, 95, 69–86.
- van der Marel, R.P., Cretton, N., de Zeeuw, P.T., & Rix, H.-W., 1997, Improved evidence for a black hole in M32 from HST/FOS spectra – II. Axisymmetric dynamical models, *ApJ*, submitted (astro-ph/9705081).
- Weinberg, M.D., 1997, The fate of cannibalized fundamental-plane elliptical galaxies, *ApJ*, 478, 435–445.
- White, S.D.M., 1983, Simulations of sinking satellites, *ApJ*, 274, 53–61.
- Wilson, A.S. & Colbert, E.J.M., 1995, The difference between radio-loud and radio-quiet active galaxies, *ApJ*, 438, 62–71.
- Xu, G. & Ostriker, J.P., 1994, Dynamics of massive black holes as a possible candidate of galactic dark matter, *ApJ*, 437, 184–193.
- Young, P.J., 1977, The black tide model of QSOs. II - Destruction in an isothermal sphere, *ApJ*, 215, 36–52.
- Young, P., 1980, Numerical models of star clusters with a central black hole. I. Adiabatic models, *ApJ*, 242, 1232–1237.
- Zhao, H.S., 1996, Analytical models for galactic nuclei, *MNRAS*, 278, 488–496.